Electronic Supplementary Material (ESI) for Nanoscale.

Supporting information

Ultra-durable Rotary Micromotors Assembled from Nanoentities by Electric Fields

*Jianhe Guo[1], Kwanoh Kim[2], Kin Wai Lei[1], and D. L. Fan[1, 2] **

[1] Materials Science and Engineering Program, the University of Texas at Austin, Austin, TX 78712, USA
[2] Department of Mechanical Engineering, the University of Texas at Austin, Austin, TX 78712, USA

*Correspondence can be addressed to: dfan@austin.utexas.edu

1. Fabrication of nanowires:

Arrays of multisegment Au/Ni/Au nanowires were fabricated by electrodeposition into nanoporous templates in a three-electrode setup. The three electrode system consists of a Cu layer on the back of polycarbonate nanoporous template as the working electrode, Pt mesh as the counter electrode, and Ag/AgCl electrode as the reference electrode. The deposition of materials was initiated from the Cu film at the bottom of nanopores, the size of which determines the diameter of the nanowires. The amount of electric charges passing through the circuit controls the length of each segment of the nanowires. As a result, arrays of nanowires can be readily synthesized. After centrifuging and dispersing in DI water and ethanol alternatively for at least two times, they were suspended in DI water.

2. Fabrication of the multi-layer magnetic nanobearings:

The patterned magnetic nanobearings were fabricated by using poly-methyl methacrylate (PMMA)/Cr templates prepared via colloidal lithography. The fabrication consists of a few steps (as shown in Fig. S1): firstly, a polystyrene (PS) nanosphere monolayer is uniformly dispersed on the surface of PMMA films. Then, a thin layer of Cr is deposited on top of the PMMA film. After the removal of the PS nanospheres and oxygen reactive ion etching (RIE) with the Cr layer as the etch mask, arrays of nanoholes can be formed on the PMMA film. Next, the multi-layer metal thin films are deposited into the nanoholes, which form into a large array of nanodisks after selective dissolution of the PMMA template. The density and size of the magnetic bearings can be well controlled by the concentration and the size of the PS nanospheres in the suspension.

3. Video analysis and speed-angle fitting

The videos recording the long-term rotation were analyzed by a professionally developed software based on classical image recognition techniques, which generates the raw data of angle versus frame. The average speeds of micromotors were calculated by linearly fitting of plots of angle versus time at tested time intervals, while the instant speeds were obtained by the first derivative of the angle-time curves. The equation (4):

$$a\omega = d\sin(\theta - \theta_M) + e\cos(\theta - \theta_M) + g + (b + c)V^2$$

could be rewritten into:

$$\omega = \frac{d}{a}\sin(\theta - \theta_M) + \frac{e}{a}\cos(\theta - \theta_M) + C, \quad S(1)$$

where $C = (g + (b + c)V^2)/a$. The constant a was calculated as $1.49 \times 10^{-20}\, N \cdot m \cdot sec/rad$ for a rotor of 165 nm-diameter Au (1.8 um)/Ni (500 nm)/Au (1.8 um) nanowire, and the magnetic orientation angles of the nanobearing θ_M were from the initial aligned angle of the rotor. With known constants of a and initial aligned angle θ_M, the value of magnetic torque amplitude *d* and frictional torque amplitude *e* could be readily obtained by fitting the speed-angle curves (20 sequential rotation cycles) with equation S(1).

4. Calculation of the amplitudes of magnetic load force, frictional force, and instant center of rotation:

The amplitude of magnetic load force is calculated according to the following equation:

$$F_M = 3\mu_0 m_1 m_2/(4\pi x^4), \quad S(2)$$

where μ_0 is the magnetic permittivity of vacuum, m_1 and m_2 are the horizontal magnetic moments of the nanowire and bearing, respectively, x is the separation distance between the magnetic moments of the nanowire and bearing that we simply consider as magnetic dipoles. With known magnetic torque and the separation distance at the beginning of the rotation, the value of $3\mu_0 m_1 m_2/(4\pi)$ can be readily calculated. For instance, it is calculated as $1.24 \times 10^{-39}\ N \cdot m^4$ for the micromotors with 500-nm-diameter Au as the top layer of the magnetic bearing. Now, with the experimentally determined time-dependent magnetic torque (F_M) and calculated value of $3\mu_0 m_1 m_2/(4\pi)$, the instant separation distance (x) can be readily determined as well as the amplitude of the angle-dependent-component of the magnetic load, given by equation (3).

The amplitude of the frictional force is estimated from $F_f = \tau_f/l$, where l is the diameter of the contact area. So the amplitudes of the frictional force could be calculated with the known frictional torque.

By overlapping two sequential frames of the recorded video of the rotating nanowire motor, the instance center of rotation of the micromotor can be found at the point of intersection of the images of the nanowire rotor.

5. Analysis of the Wear of the Nanorotors and Bearings in Terms of Center of rotation, Materials, and Fabrication Methods:

We designed micromotors with the length of the Ni segments of the nanowires same as the diameters of magnetic nanobearings so that Ni segments could be in full contact with Au spacer layer during rotation. However, the rotation of rotors may not always perfectly center on the bearings. It could be due to the strong magnetic dipole interaction between tips of the magnetic segment of the nanowire and edge of the magnetic bearing, which causes the rotation of magnetic segment off the center. From the distribution of the rotation center of the micromotor in Fig. 3(b), we can find two extremes: (1) rotation at the center, (2) rotation around the edge. If the rotation center is at the center of the bearing, Ni segment is always on Au during the entire rotation cycle. If it is at the edge, we can say that the Ni segment is on Au for at least 50% of a rotation cycle. Therefore, we could roughly estimate that Ni is in full contact with Au for 75% of the rotation time. Although there is a certain extent of Au-on-Au contact during the rotation, neither Ni nor Au segments on the rotors has clearly observable wear according to our SEM characterization (Fig. S2). We attribute this to two factors: (1) it is found that the hardness of electroplated Au (~80 HV) can be 33% higher than that of the high-vacuum evaporated Au (~60 HV) due to impure elements incorporated during the electrodeposition process.[1,2] Also when making the multisegment nanowires, we altered electrolytes in the same container, although after careful washing with D. I. water. These factors both make the Au segments in the nanowires less pure and harder than that of evaporated Au; (2) the intermetallic diffusion at the interface of Au and Ni segments of the nanowire can greatly enhance the hardness of Au next to the Ni segment. It is reported that 1 wt% Ni could increase the hardness of Au by 30% and 2 wt %

Ni could increase the hardness by 80%.[3,4] The hardness of electroplated Ni (200-500 HV) is higher than that of either electrodeposited or evaporated Au.[5]

References:

(1) Baker, R. G.; Palumbo, T. A. The Case for End-Point Requirements in Gold Plating Specifications for Electronic Equipment. *Plating* **1971**, 58, 791-800.
(2) Miyoshi, K.; Buckley, D. H.; Spalvins, T. Friction and hardness of gold films deposited by ion plating and evaporation; National Aeronautics and Space Administration, Scientific and Technical Information Branch, United States, 1983.
(3) Liljestrand, L. G; Sjogren, L; Revay, L; Asthner, B. Wear Resistance of Electroplated Nickel-Hardened Gold. *IEEE Trans. Compon., Hybrids, Manuf. Technol.* **1985**, 8, 123-128.
(4) Dini, J. W. Electrodeposition—the materials science of coatings and substrates; Noyes Publications: Park Ridge, NJ, 1993.
(5) Nakano, H.; Tsuji, H.; Oue, S.; Fukushima, H.; Yang, F.; Tian, W. Effect of Organic Additives on the Hardness of Ni Electrodeposited from Sulfamate and Watt's Solutions. *Mater. Trans.* **2011**, 52, 2077-2082.

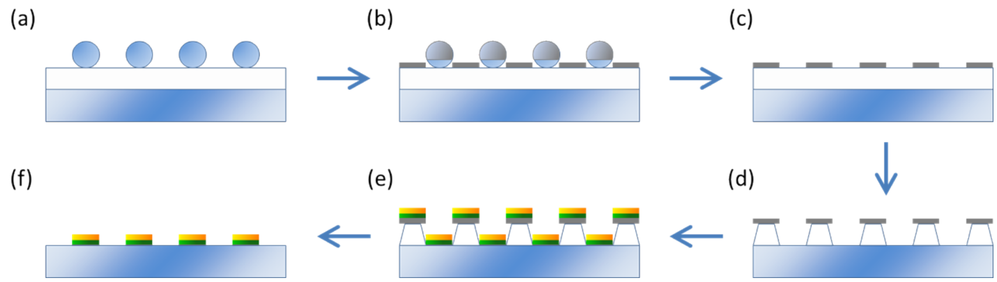

Figure S1. Fabrication of tri-layer magnetic disks as bearings of micromotors: (a) a polystyrene (PS) nanosphere monolayer is uniformly dispersed on the surface of PMMA thin film [white] on a substrate; (b) a thin film of Cr [gray] is deposited on top of PMMA; (c – d) after the removal of the PS nanospheres, arrays of nanoholes can be formed on the PMMA film after reactive oxygen ion etching with the Cr pattern as an etch mask; (e) Cr [gray] /Ni [green] /Au [yellow] thin films are deposited sequentially into the nanoholes and form into an array of magnetic disks; (f) finally, the PMMA is dissolved and arrays of Au/Ni/Cr nanodisks can be formed as bearings for micromotors.

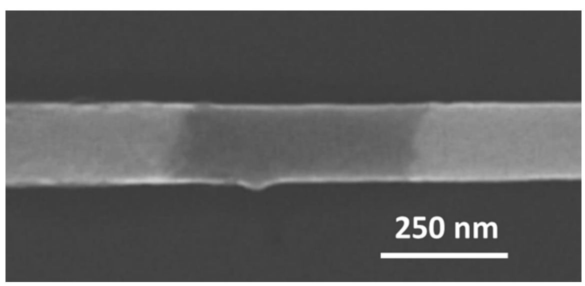

Figure S2. Scanning electron micrographs of nanowires after 22.6-hour rotation.

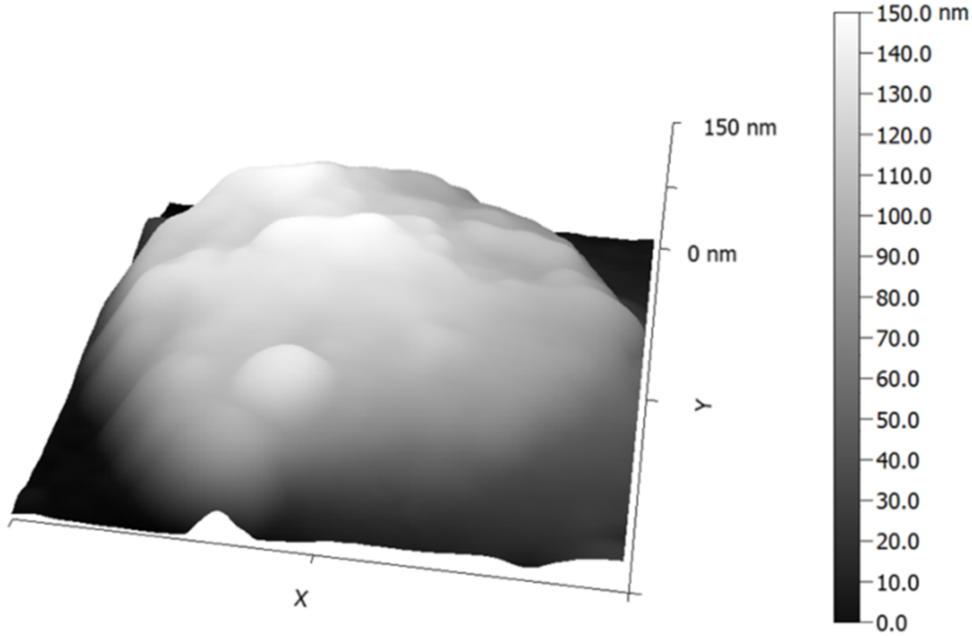

Figure S3. AFM image obtained by taping mode showing the wear of the magnetic bearing [Au (60 nm)/Ni (80 nm)/Cr (6 nm)] after 22 hour rotation. The average thickness of Au at the bottom right of the bearing, which is the most worn region, is 26 nm. (Obtained from the AFM software Gwyddion, based on the known thickness of Ni and Cr)

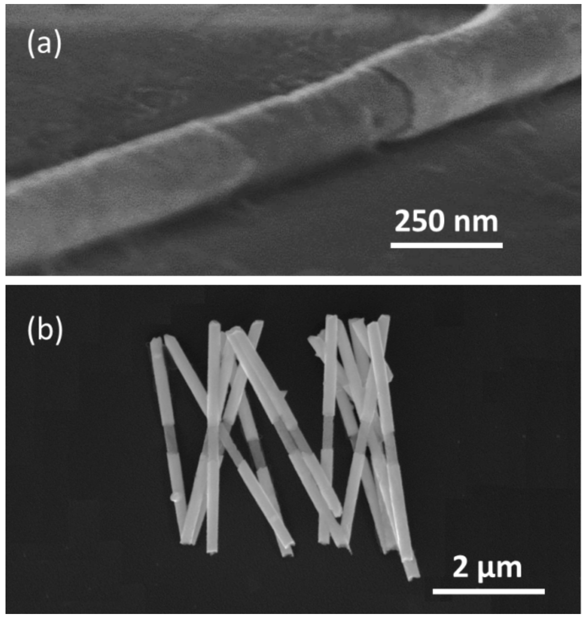

Figure S4. (a) SEM image of nanowire after 80-hour rotation. (b) Non-rotated nanowires in the same suspension.

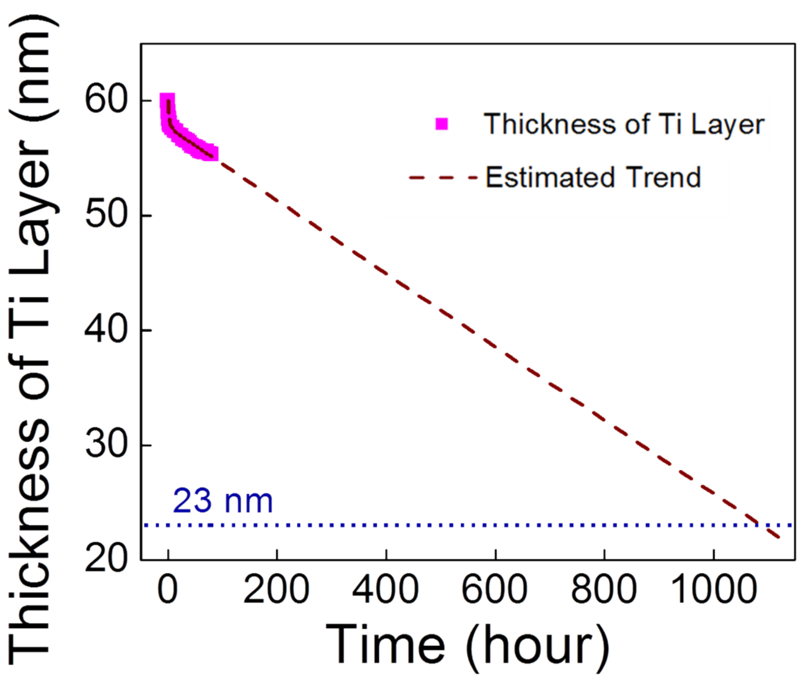

Figure S5. Extrapolation of the curve of thickness of Ti versus rotation time for estimation of the device life time. Since there is a 6 nm Cr layer between the Ti and Ni layer, the final thickness of Ti is set as 23 nm.

Video S1. Rotation of micromotors with Au supported bearing for 22.6 hour.

Video S2. Rotation of micromotors with Ti supported bearing both clockwise and counterclockwise for 80 hours in total.